Annual Review 2004

神経

編集
柳澤信夫　関東労災病院院長
篠原幸人　東海大学教授
岩田　誠　東京女子医科大学教授
清水輝夫　帝京大学教授
寺本　明　日本医科大学教授

中外医学社

起立性低血圧の機序と治療

高知医科大学循環制御学教授　佐藤隆幸

key words　baroreflex, supine hypertension, orthostatic hypotension, bionic baroreflex

動　向

自律神経疾患における起立性低血圧は，重症になると意識障害を引き起こすため，しばしば寝たきりの原因となり，生活の質を著しく損なう．また寝たきりから嚥下性肺炎を合併し，生命をもおびやかすきわめて重要な病態である．また，これまで，あまり注目されていなかった自律神経疾患における臥位高血圧を伴う起立性低血圧という複雑な病態を呈する症例がかなり多いこともわかってきた．臥位高血圧は起立性低血圧を悪化させる要因であることから，精力的にその病態を理解する試みがなされつつある．

一方，治療に関しては，残念ながら大きな進展はなかった．起立性低血圧が圧受容器反射の機能障害を基盤としていることから考えても，従来の薬物療法による静的な治療には自ずから限界がある．すなわち，圧受容器反射が動的（ダイナミック）機能であることから，動的あるいはオンデマンド（on demand）的な治療体系が必要であろう．骨格筋や交感神経の電気刺激を必要に応じて行うフィードバック型の治療体系の創出が期待されている．

A. 起立性低血圧の機序

自律神経機能を評価する場合，Valsalva試験・寒冷昇圧試験・心拍変動のスペクトル解析など循環動態に関する情報を用いることが多い[1]．このことは，循環動態の制御に自律神経がいかに重要であるかを物語っている．なかでも，起立負荷は，日常生活の中で繰り返される体位変換そのものであり，これに対する異常応答，すなわち起立性低血圧は，生活の質を損なう重要な病態である．しかしながら，この病態は，未解明な点が多く，自律神経学と循環器学にまたがる学際的な研究が日夜精力的に行われ，新たな知見が加えられつつある．ここでは，まず正常な起立時の血圧維持機構に触れ，最新の知見を紹介する．

ヒトが起立すると循環血液量の分布は大きな偏りを生じる．重力により500ないし700mlの血液が胸腔から下方の下肢や腹部臓器などに移動し，心臓への還流血液量が約30%減少するため心拍出量は減少する．このため心房レベルを基準として測定される血圧は大きく低下する．この短時間に生ずる循環動態の急激な変化に対して，圧受容器反射がその変化をうち消すようにはたらくため，健常者では血圧の低下は20mmHg以内にとどまる．

1. 圧受容器反射に関する最近の知見

圧受容器反射は，頚動脈洞や大動脈弓部に存在する圧受容器，延髄をはじめとする脳幹部に存在する血管運動中枢，交感神経遠心路，効果器である心血管系からなるフィードバック調節システムである．圧受容器は血圧による血管壁の機械的伸展を感知し，舌咽神経や迷走神経の求心路を介してその情報を中枢に伝える．血管運動中枢には，この他に，呼吸中枢からの入力や大脳皮質からのいわゆるcentral commandなども入力されているが，これらの情報を統合し，その出力は，脊髄中間質外側核の交感神経節前線維に伝えられる．その後この血管運動性交感神経活動は，多くの場合，交感神経節で節後線維に伝達された後，血圧調節に重要な細動脈や細静脈の接合部に達する．細動脈は抵抗血管としてはたらき，血管抵抗を決定する．一方，細静脈は，容量血管としてはたらき，静脈還流を決定する．

以上のように圧受容器反射の各要素における機能については，これまでによく理解されていた．しかしながら，これらの知見を臨床に応用して，定量的かつ解析的に圧受容器反射の機能を評価する枠組みはなかった．Satoらは，最近，平衡線図解析法により，圧受容器反射の機能を解析的に評価する手法を提案している[2]．フィードバック調節システムである圧受容器反射は，図1のように，圧受容器で検知される血圧が交感神経活動を決定するまでの制御部と，交感神経活動から血圧が決定される制御対象部の2つのサブシステムに単純化することができる．圧受容器反射で決定される血圧はそれぞれのサブシステムの機能特性曲線が交差する平衡点である，とするこの枠組みは，起立性低血圧の機序を大きく2つに類型することを可能にし，かつ圧受容器反射の機能を定量的にとらえる基盤となりうる．図2に示されているように，健常例では，起立により，制御対象部の機能曲線が下方偏位しても，血圧の低下はある程度抑制される．しかし，制御部の機能不全や制御対

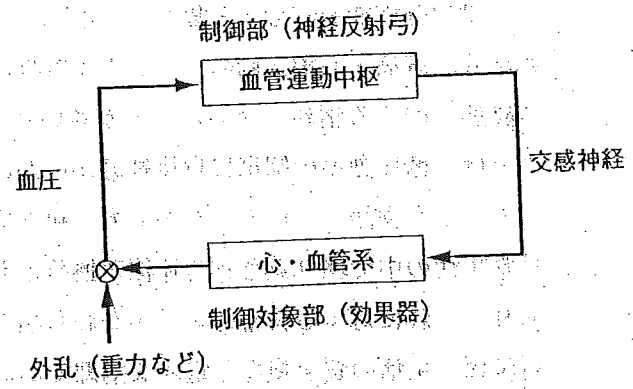

図1　圧受容器反射のブロック線図
ブロック線図は，生体内の情報の流れを図示したもので，圧受容器反射は制御部と制御対象部の2つのサブシステムに分けることができる．

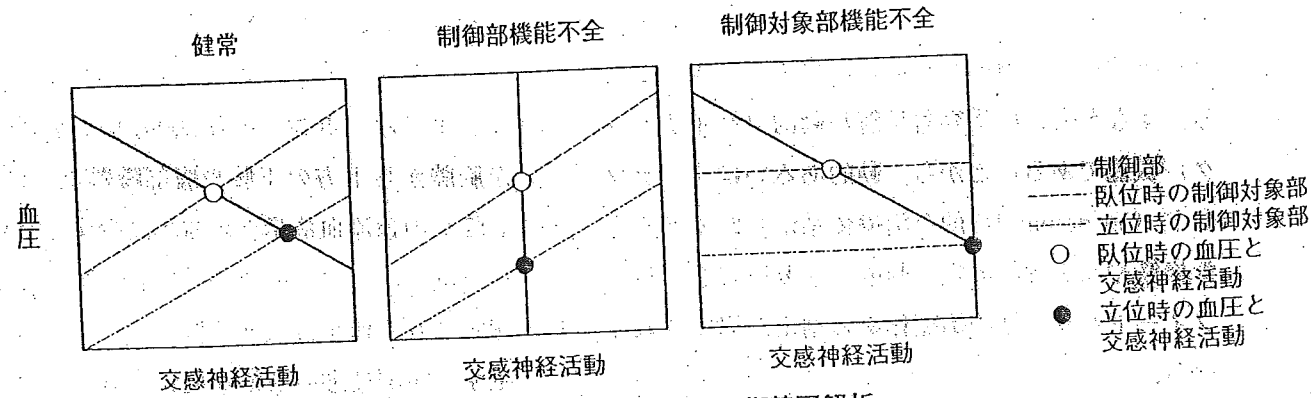

図2　圧受容器反射の平衡線図解析
縦軸は血圧，横軸は交感神経活動である．制御部の機能特性は，血圧（圧受容器圧と等しい）を入力交感神経活動を出力とした入出力関係で示される．制御対象部の機能特性は，入力を交感神経活動，出力を血圧とした入出力関係で示される．

象部の機能不全では，起立に伴って，血圧が大きく低下することが平衡線図から容易に理解することができる．すなわち，制御部機能不全の場合，圧受容器圧の変化に対して，交感神経活動が無反応であるため，制御部の機能曲線は平衡線図上，垂直の直線になるため，起立に伴う制御対象部の偏位分がそのまま血圧の低下として現れてしまう．また，制御対象部の機能不全では，交感神経活動に対する血圧応答がみられないため，平衡線図上では，制御対象部の機能曲線が水平の直線になる．したがって，起立に伴う制御対象部の偏位が直接的に血圧の低下につながる．今後，このような解析的枠組みを用いて，起立性低血圧の定量的な病態生理学的分類がなされることが期待される．

2. 自律神経疾患における臥位高血圧

起立性低血圧をきたす自律神経疾患では，しばしば臥位高血圧を伴うことが知られているが，その重要性に関しては充分には認識されていない[3-5]．しかし，臥位高血圧は，起立性低血圧治療のために用いられる昇圧薬の投与を困難にしたり，また，臥床時の圧利尿による脱水がさらに起立性低血圧を増悪させるため，きわめて重要な病態であると考えられる[6,7]．

Shannonらは，多系統萎縮症 multiple system atrophy（MSA）と純粋性進行性自律神経失調症 pure progressive autonomic failure（PAF）の患者を対象とした薬理学的アプローチにより，これらの自律神経疾患における臥位高血圧と残存する交感神経活動との関連について調査した[8]．MSAでは，安静臥位時の血漿ノルエピネフリン濃度の高値が約半数にみられ，節遮断薬トリメタファン投与により血漿ノルエピネフリン濃度と血圧が用量依存的に低下することをみいだした．トリメタファン投与による血圧低下は60ないし130mmHgにも及んだ．一方，PAFは安静時の血漿ノルエピネフリン濃度が低値で，トリメタファンによる血圧低下も10 mmHg程度であった．これらの結果は，MSAにおける臥位高血圧に残存交感神経活動が関与していることを示唆している．また，彼らは，MSAにおいて血漿ノルエピネフリン濃度が高値である症例では，圧受容器からの求心路障害が関与している可能性があると考えている．一方，PAFにおける臥位高血圧の機序は不明であった．

3. 下肢における血液貯留

自律神経疾患における起立性低血圧の機序として，起立性交感神経緊張による血管収縮の障害が重要であることは一致した意見であったが，血行動態的にみた場合，その障害が抵抗血管の異常応答として現れるのか，容量血管の異常として現れるのかはっきりしていなかった[9]．

Brownらは，家族性自律神経失調症 familial dysautonomia（FD）を対象に，総末梢血管抵抗と下腿容積の起立負荷に対する応答を測定した[10]．その結果，総末梢血管抵抗は，健常者では40%の増大がみられるにもかかわらず，FDでは無反応であった．一方，下腿容積の増大は健常者と同様にFDでも数%以内であった．このようなことから，自律神経疾患における起立負荷に対する血行動態の応答異常は，総末梢血管抵抗が増大しないことであり，下腿への血液貯留ではないと判断した．すなわち起立負荷に対する交感神経を介する血管収縮の障害の主座は，細動脈であると考えられた．自律神経疾患で下腿容積が増大しなかった理由として，筋原性の静脈収縮の機能が温存されている可能性を示唆した．しかしながら，これらの結果は，起立負荷後10分という短期応答であるため，細動脈収縮障害により，二次的に下腿静脈へ血液貯留を生ずる可能性を否定できない．

Stewartも，体位性頻脈症候群 postural tachycardia syndrome（POTS）を対象に，同様の研

究を行い，下腿血管の起立負荷に対する応答異常は，細動脈にみられ，静脈の圧-容積関係には異常がみられないと報告し，POTSにおける下肢への血液貯留が起立に対する静脈の異常応答であるという説を否定している[11]．

4. 脳血流異常

自律神経疾患における脳血流の自動調節能の障害と起立性低血圧との関連を示唆する報告があるが，一定の知見は得られていない．Hesseらは，自律神経疾患を対象に陽電子放射断層撮影法positron emission tomography（PET）を用いて，脳血流の自動調節能について調査した．ノルアドレナリンによる昇圧および下半身陰圧装置による降圧時の血圧-脳血流関係から，脳血流の自動調節能を評価したが，疾患群に一致する結果を得ることはできなかった[12]．今後さらに検討が必要である．

5. 臥床の影響

自律神経疾患における起立性低血圧は朝方により悪化する．その一因として，しばしば合併する臥位高血圧による圧利尿が循環血液量の減少を引き起こすことがあげられている．Ombonіらは，自律神経疾患を対象に夜間就寝前と早朝起床時に血行動態を比較した[6]．その結果，臥位血圧は就寝前と起床時で差がなかったが，立位での血圧降下は起床時に著しかった．同時に計測した血管抵抗は，就寝前立位と起床時立位で有意な差がみられなかった．一方，起床時立位の心拍出量は就寝前立位のそれよりも有意に減少していた．就寝前と起床時で有意な体重減少はみられなかった．このようなことから，体液の血管外への移動が夜間臥床時に生ずるため，起立性低血圧が起床時に悪化すると結論づけている．

6. 遺伝子多型

Tabaraらは，地域の50歳以上の住民を対象にした健診時に得られたデータと血液サンプルを用いた研究により，起立に伴う収縮期血圧の降下度と交感神経系とレニン-アンジオテンシン系の遺伝子多型の相関を調査した[13]．その結果，起立に伴う収縮期血圧の降下度と交感神経の効果器における情報伝達と密接に関係するGs蛋白の遺伝子多型との有意な関連をみいだしたが，アンジオテンシン変換酵素，アンジオテンシノーゲンあるいはアンジオテンシン受容体の遺伝子多型とは有意な関連が認められなかった．これらの結果は，圧受容器反射における制御対象部の機能特性に遺伝的背景があることを示唆するもので大変興味深い．

B. 起立性低血圧の治療

起立性低血圧の根本的な治療は，圧受容器反射の機能を回復あるいは再建することである．

1. 薬物療法

L-threo-DOPS，fludrocortisone，midodrineなど従来報告されているもの以外に特に目新しい薬物療法は報告されていないが[14-16]，Kawakamiらは，貧血を合併していない家族性アミロイドーシスにおける起立性低血圧にエリスロポエチンの投与が有効であったという症例を報告している[17]．興味ある研究であるが，その作用機序については不明である．

2. 飲　水

Shannonらは，飲水（5分以内に480mlを摂取）の昇圧作用について報告している．自律神経失調症を対象に立位で飲水させ，経時的に血圧の変化を記録したところ，飲水直後より血圧は上昇し，飲水開始後30分には，約30mmHgの昇圧がみら

れた[18]．Tankらは，その作用機序の1つとして残存する脊髄反射機能を想定しているが[19]，詳細は今後の課題である．いずれにしても，その反応が迅速で，比較的作用時間が長いことから，補助的な治療法として有用かもしれない．

3. 腹筋および下肢筋肉の電気刺激

自律神経疾患ではないが，外傷性脊髄損傷の症例を対象に表面電極を用いた腹筋[20]や下肢筋肉[21]の電気刺激により昇圧可能であることが報告されている．脊髄損傷患者における食後低血圧の治療への応用が期待されているが，同様に，自律神経疾患における起立性低血圧にも応用可能であると思われる．

4. バイオニック圧受容器反射システム

圧受容器反射を機能的に再建する手段として，交感神経を電気刺激するフィードバック血圧制御装置が開発されつつある[22,23]．図3に示されているように，圧センサー，コンピュータ，電気刺激装置，刺激電極からなるシステムで，コンピュータには，血管運動中枢の機能を代行するロジックがプログラムされている．動物実験では，図4のように圧受容器反射失調による起立性低血圧に有効であることが報告されている．今後の展開が期待される．

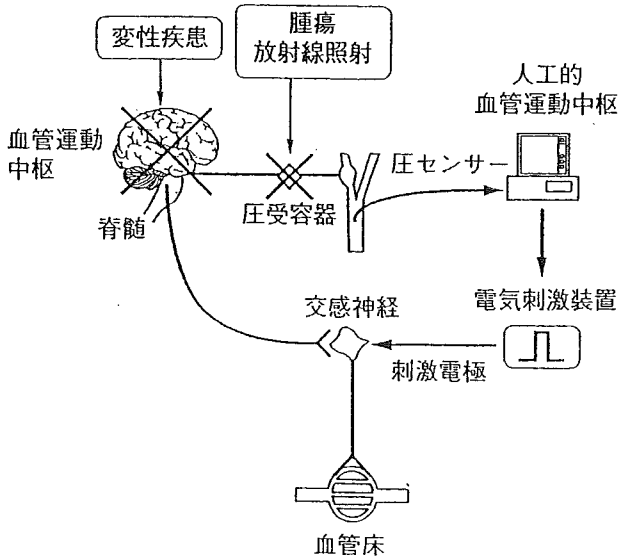

図3　バイオニック圧受容器反射装置の概略

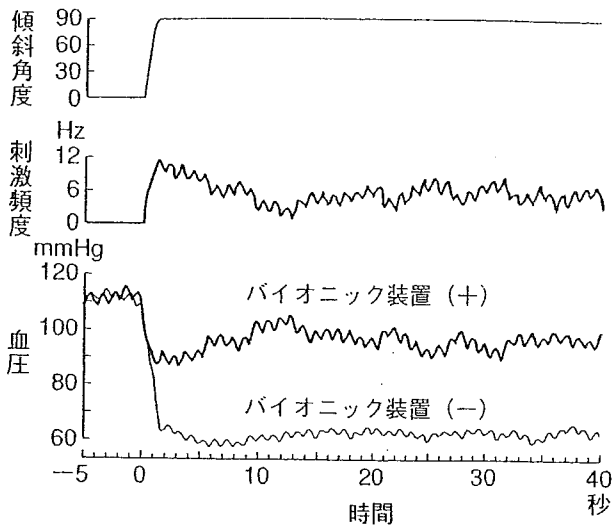

図4　バイオニック装置による圧受容器反射失調の機能再建例

圧受容器反射機能が廃絶したラットにバイオニック装置を埋め込んで機能再建すると，head-up tiltに伴う急激な血圧低下がくい止められる．

文献

1) 自律神経学会編．自律神経機能検査 第3版．東京：文光堂；2000.
2) Sato T, Kawada T, Inagaki M, et al. A new analytical framework for understanding the sympathetic baroreflex control of arterial pressure. Am J Physiol 1999; 276: H2251-61.
3) Jordan J, Biaggioni I. Diagnosis and treatment of supine hypertension in autonomic failure patients with orthostatic hypotension. J Clin Hypertens 2002; 4: 139-45.
4) Bioggioni I, Robertson RM. Hypertension in orthostatic hypotension and autonomic dysfunction. Cardiol Clin 2002; 20: 291-301.
5) Goldstein DS, Pechnik S, Holmes C, et al. Association between supine hypertension and orthostatic hypotension in autonomic failure. Hypertension 2003; 42: 136-42.
6) Omboni S, Smit AA, van Lieshout JJ, et al. Mechanisms underlying the impairment in orthostatic tolerance after nocturnal recumbency in patients with autonomic failure. Clin Sci (Lond) 2001; 101: 609-18.

7) Hao WY, Bai J, Wu XY, et al. Simulation study of the effects of hypovolemia on cardiovascular response to orthostatic stress. Med Biol Eng Comput 2003; 41: 44-51.
8) Shannon JR, Jordan J, Diedrich A, et al. Sympathetically mediated hypertension in autonomic failure. Circulation 2000; 101: 2710-5.
9) Chandler MP, Mathias CJ. Haemodynamic responses during head-up tilt and tilt reversal in two groups with chronic autonomic failure: pure autonomic failure and multiple system atrophy. J Neurol 2002; 249; 542-8.
10) Brown CM, Stemper B, Welsch G, et al. Orthostatic challenge reveals impaired vascular resistance control, but normal venous pooling and capillary filtration in familial dysautonomia. Clin Sci (Lond) 2003; 104: 163-9.
11) Stewart JM. Pooling in chronic orthostatic intolerance: arterial vasoconstrictive but not venous compliance defects. Circulation 2002; 105: 2274-81.
12) Hesse B, Mehlsen J, Boesen F, et al. Regulation of cerebral blood flow in patients with autonomic dysfunction and severe postural hypotension. Clin Physiol Funct Imaging 2002; 22: 241-7.
13) Tabara Y, Kohara K, Miki T. Polymorphisms of genes encoding components of the sympathetic nervous system but not the renin-angiotensin system as risk factors for orthostatic hypotension. J Hypertens 2002; 20: 651-6.
14) Mathias CJ, Senard JM, Braune S, et al. L-threo-dihydroxyphenylserine (L-threo-DOPS; droxidopa) in the management of neurogenic orthostatic hypotension: a multi-national, multi-center, dose-ranging study in multiple system atrophy and pure autonomic failure. Clin Auton Res 2001; 11: 235-42.
15) Oldenburg O, Kribben A, Baumgart D, et al. Treatment of orthostatic hypotension. Curr Opin Pharmacol 2002; 2: 740-7.
16) Frishman WH, Azer V, Sica D. Drug treatment of orthostatic hypotension and vasovagal syncope. Heart Dis 2003; 5: 49-64.
17) Kawakami K, Abe H, Harayama N, et al. Successful treatment of severe orthostatic hypotension with erythropoietin. Pacing Clin Electrophysiol 2003; 26 (1 Pt 1): 105-7.
18) Shannon JR, Diedrich A, Biaggioni I, et al. Water drinking as a treatment for orthostatic syndromes. Am J Med 2002; 112: 355-60.
19) Tank J, Schroeder C, Stoffels M, et al. Pressor effect of water drinking in tetraplegic patients may be a spinal reflex. Hypertension 2003; 41: 1234-9.
20) Taylor PN, Tromans AM, Harris KR, et al. Electrical stimulation of abdominal muscles for control of blood pressure and augmentation of cough in a C3/4 level tetraplegic. Spinal Cord 2002; 40: 34-6.
21) Faghri PD, Yount J. Electrically induced and voluntary activation of physiologic muscle pump: a comparison between spinal cord-injured and able-bodied individuals. Clin Rehabil 2002; 16: 878-85.
22) Sato T, Kawada T, Shishido T, et al. Novel therapeutic strategy against central baroreflex failure: a bionic baroreflex system. Circulation 1999; 100: 299-304.
23) Sato T, Kawada T, Sugimachi M, et al. Bionic technology revitalizes native baroreflex function in rats with baroreflex failure. Circulation 2002; 106: 730-4.

116 Bionic Baroreflex

Takayuki Sato
Department of Cardiovascular Control
Kochi Medical School
Kochi, Japan

André Diedrich
Division of Clinical Pharmacology
Vanderbilt University
Nashville, Tennessee

Kenji Sunagawa
Department of Cardiovascular Dynamics
National Cardiovascular Center Research Institute
Osaka, Japan

A novel therapeutic strategy against central baroreflex failure is proposed on the basis of bionic technology. A recent innovation, bionic baroreflex system (BBS), was achieved to revitalize baroreflex function through a neural interface approach. In the BBS, arterial pressure is sensed through a micromanometer placed in the aortic arch and fed into a computer ambitious of functioning as an artificial vasomotor center. On the basis of measured changes in arterial pressure, the artificial vasomotor center commands an electrical stimulator to provide a stimulus of the appropriate frequency to the vasomotor sympathetic nerves. Although the BBS is not currently available for clinical practice, the future advance in its development is expected.

The arterial baroreflex is the most important negative feedback system to suppress the effects of rapid daily disturbances in arterial pressure [1]. Therefore, in patients with autonomic failure without baroreflex control of arterial pressure, the simple act of standing would cause a decrease in arterial pressure, reducing perfusion of the brain, and resulting potentially in loss of consciousness. The functional restoration of the arterial baroreflex is essential to patients with baroreflex failure caused by autonomic failure.

In patients with central baroreflex failure such as baroreceptor deafferentation, Shy–Drager syndrome, and spinal cord injuries, peripheral sympathetic nerves are still functional but not controlled by the brain. A novel therapeutic strategy has been proposed to use a BBS with a neural interface approach to control arterial pressure [2, 3]. A bionic system is an artificial device for functional replacement of a physiologic system able to mimic its static and dynamic characteristics. In the proposed BBS (Fig. 116.1), arterial pressure is sensed through a micromanometer placed in the aortic arch and fed into a computer ambitious of functioning as an artificial vasomotor center. On the basis of measured changes in arterial pressure, the artificial vasomotor center commands an electrical stimulator to provide a stimulus of the appropriate frequency to the vasomotor sympathetic nerves. This recent innovation, BBS, was achieved to revitalize baroreflex function in an animal model of central baroreflex failure.

BIONIC BAROREFLEX SYSTEM

Theoretic Background

It is of critical importance to identify the algorithm of the artificial vasomotor center—that is, how to determine the stimulation frequency (STM) of the vasomotor sympathetic nerves in response to changes in arterial pressure (AP). On the basis of expertise of bionics and systems physiology, the algorithm has been determined as transfer function by a white-noise system identification method [2]. First, the functional characteristics to be mimicked by the BBS—that is, the open-loop transfer function of native baroreflex (H_{native})—is identified in healthy subjects (Fig. 116.2). Second, the open-loop transfer function of the AP response to STM ($H_{STM \rightarrow AP}$) is determined in patients with central baroreflex failure. Finally, a simple process of division, $H_{Native}/H_{STM \rightarrow AP}$, could yield the transfer function required for the artificial vasomotor center of the BBS—that is, $H_{AP \rightarrow STM}$.

Implementation of Algorithm of Artificial Vasomotor Center in Bionic Baroreflex System

To operate in real time as the artificial vasomotor center, the computer was programmed to automatically calculate instantaneous STM in response to instantaneous AP changes according to a convolution algorithm [2, 3]:

$$STM(t) = \int_0^{\infty} h(\tau) \cdot AP(t - \tau)\, d\tau$$

where $h(t)$ is an impulse response function computed by an inverse Fourier transform of $H_{AP \rightarrow STM}$.

Efficacy of Bionic Baroreflex System

In a prototype of the BBS for rats with central baroreflex failure, the celiac ganglion was selected as the sympathetic vasomotor interface [3]. The efficacy of the BBS against orthostatic hypotension during head-up tilting (HUT) is shown in Figure 116.3. Without the activation of the BBS, HUT produced a rapid progressive decrease in AP by

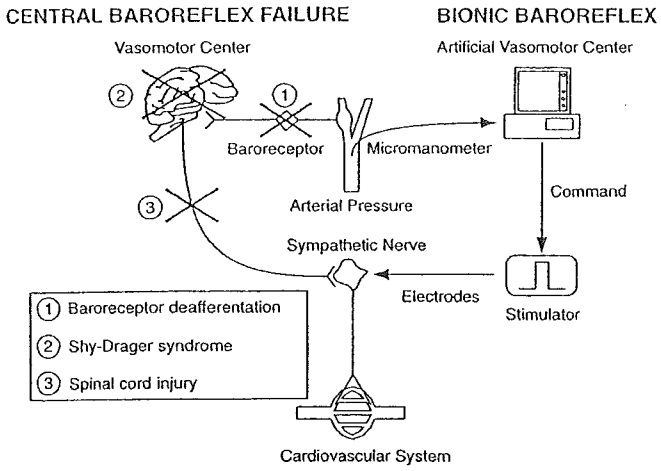

FIGURE 116.1 Central baroreflex failure and its functional replacement by a bionic baroreflex system.

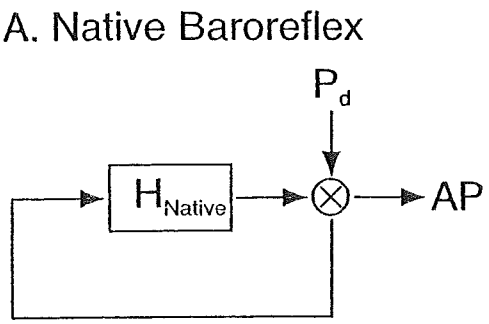

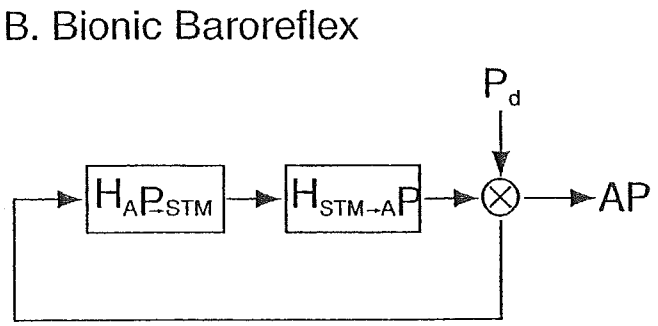

FIGURE 116.2 Block diagrams of native and bionic baroreflex systems. H_{Native} denotes the open-loop transfer function of the native baroreflex system. $H_{AP\text{-}STM}$ and $H_{STM\text{-}AP}$ are the open-loop transfer functions from arterial pressure (AP) to the frequency of electrical stimulation (STM) and from STM to AP, respectively. P_d is an external disturbance in pressure. (Modified from Sato, T., T. Kawada, M. Sugimachi, and K. Sunagawa. 2002. Bionic technology revitalizes native baroreflex function in rats with baroreflex failure. *Circulation* 106:730–734.)

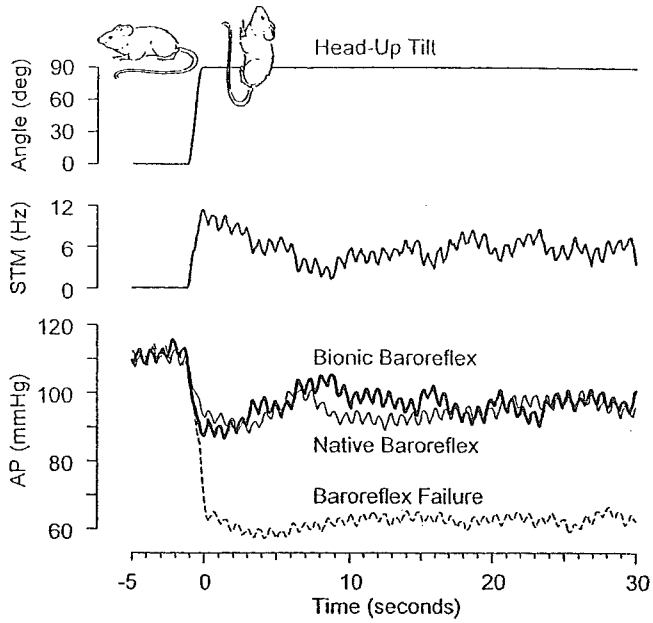

FIGURE 116.3 Real-time operation of the bionic baroreflex system during head-up tilting (HUT). In a model of central baroreflex failure (*broken line*), when the bionic baroreflex system was inactive, arterial pressure (AP) decreased rapidly and severely immediately after HUT. Conversely, whereas the bionic baroreflex system was activated (*thick line*), such an AP decrease was buffered as if the native baroreflex function (*thin line*) was restored. Although sensing changes in AP, the bionic baroreflex system automatically computed the frequency of electrical stimulation (STM) of the sympathetic nerves and drove a stimulator. (Modified from Sato, T., T. Kawada, M. Sugimachi, and K. Sunagawa. 2002. Bionic technology revitalizes native baroreflex function in rats with baroreflex failure. *Circulation* 106:730–734.)

40 mmHg only in 2 seconds. In contrast, whereas the BBS was activated, it automatically computed STM and appropriately stimulated the sympathetic nerves to quickly and effectively attenuate the AP decrease. Such an AP response to HUT during the real-time execution of the BBS was indistinguishable from that during functioning of the native baroreflex system. Therefore, the BBS was considered to revitalize the native baroreflex function.

EPIDURAL CATHETER APPROACH FOR HUMAN BIONIC BAROREFLEX SYSTEM

To apply BIONIC technology to patients, a neural interface with quick and effective controllability of AP in humans is needed. Here we proposed an epidural catheter approach for the human BBS [4]. We percutaneously placed an epidural catheter with a pair of electrodes at the level of Th9-11, and then we randomly altered the stimulation frequency between 0 and 20 Hz (Fig. 116.4A). The step response computed by the transfer function analysis showed that AP

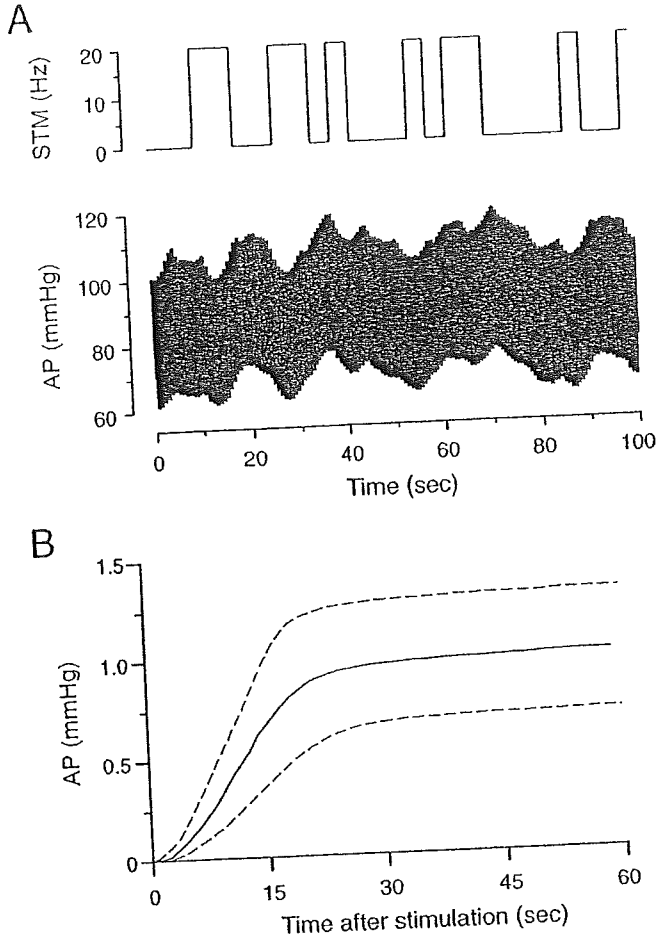

FIGURE 116.4 The response of arterial pressure (AP) to spinal cord stimulation at Th9-11 (**A**) and the step response estimated from the transfer function analysis (**B**).

quickly responded to the electrical stimulation and reached 90% of the steady-state response at 21 ± 5 seconds (see Fig. 116.4B). The gain was 1.0 ± 0.3 mmHg/Hz. Therefore, the epidural approach would be a potential interface for the human BBS.

CLINICAL IMPLICATIONS

For practical use of the BBS for patients with central baroreflex failure, clinically applicable materials and devices should be developed—that is, a pressure sensor, an implantable stimulator, and stimulating electrodes. Fortunately, certain difficulties posed by these challenges have been already addressed in other areas of clinical practice to some degree, and may be readily adaptable for use with the BBS. For example, a tonometer has been developed as a noninvasive continuous monitor of AP [5]. Implantable pulse generators such as cardiac pacemakers can serve as permanent electrical stimulators. Also, implantable wire leads for nerve stimulation and epidural catheters for spinal stimulation have been approved for the long-term treatment of some neurologic disorders [6].

References

1. Sato, T., T. Kawada, M. Inagaki, T. Shishido, H. Takaki, M. Sugimachi, and K. Sunagawa. 1999. New analytic framework for understanding sympathetic baroreflex control of arterial pressure. *Am. J. Physiol. Heart Circ. Physiol.* 276:H2251–H2261.
2. Sato, T., T. Kawada, T. Shishido, M. Sugimachi, J. Alexander, Jr., and K. Sunagawa. 1999. Novel therapeutic strategy against central baroreflex failure: A bionic baroreflex system. *Circulation* 100:299–304.
3. Sato, T., T. Kawada, M. Sugimachi, and K. Sunagawa. 2002. Bionic technology revitalizes native baroreflex function in rats with baroreflex failure. *Circulation* 106:730–734.
4. Sato, T., M. Ando, and F. Yamasaki. 2002. New potential interface of bionic system for revitalization of baroreflex function: Epidural catheter approach in humans. *Circulation* 106(Suppl II):II–110.
5. Sato, T., M. Nishinaga, A. Kawamoto, T. Ozawa, and H. Takatsuji. 1993. Accuracy of a continuous blood pressure monitor based on arterial tonometry. *Hypertension* 21:866–874.
6. Shimoji, K., H. Kitamura, E. Ikezono, H. Shimizu, K. Okamoto, and Y. Iwakura. 1974. Spinal hypalgesia and analgesia by low-frequency electrical stimulation in the epidural space. *Anesthesiology* 41:91–94.

Am J Physiol Regul Integr Comp Physiol 285: R262–R270, 2003;
10.1152/ajpregu.00692.2001.

innovative methodology

Dynamics of sympathetic baroreflex control of arterial pressure in rats

Takayuki Sato,[1,2] Toru Kawada,[1] Masashi Inagaki,[1] Toshiaki Shishido,[1] Masaru Sugimachi,[1] and Kenji Sunagawa[1]

[1]Department of Cardiovascular Dynamics, National Cardiovascular Center Research Institute, Suita, Osaka 565-8565, and [2]Department of Cardiovascular Control, Kochi Medical School, Nankoku, Kochi 783-8505, Japan

Submitted 19 November 2001; accepted in final form 10 March 2003

Sato, Takayuki, Toru Kawada, Masashi Inagaki, Toshiaki Shishido, Masaru Sugimachi, and Kenji Sunagawa. Dynamics of sympathetic baroreflex control of arterial pressure in rats. *Am J Physiol Regul Integr Comp Physiol* 285: R262–R270, 2003; 10.1152/ajpregu.00692.2001.—By a white noise approach, we characterized the dynamics of the sympathetic baroreflex system in 11 halothane-anesthetized rats. We measured sympathetic nerve activity (SNA) and systemic arterial pressure (SAP), while carotid sinus baroreceptor pressure (BRP) was altered randomly. We estimated the transfer functions from BRP to SNA (mechanoneural arc), from SNA to SAP (neuromechanical arc), and from BRP to SAP (total arc). The gain of the mechanoneural arc gradually increased about threefold as the frequency of BRP change increased from 0.01 to 0.8 Hz. In contrast, the gain of the neuromechanical arc rapidly decreased to 0.4% of the steady-state gain as the frequency increased from 0.01 to 1 Hz. Although the total arc also had low-pass characteristics, the rate of attenuation in its gain was significantly slower than that of the neuromechanical arc, reflecting the compensatory effect of the mechanoneural arc for the sluggish response of the neuromechanical arc. We conclude that the quantitative estimation of the baroreflex dynamics is vital for an integrative understanding of baroreflex function in rats.

baroreflex sensitivity; dynamic system; feedback system; mechanoneural arc; neuromechanical arc

THE MOST UNIQUE FUNCTION of arterial baroreflex is to quickly and sufficiently attenuate the effect of an external disturbance on arterial pressure (19). For example, the change in arterial pressure induced by a postural change from lying to standing is sensed by arterial baroreceptors located within the walls of the aortic arch and internal carotid arteries. This fall in pressure is neurally encoded and relayed via afferent pathways to a brain stem vasomotor center and then immediately causes an appropriate degree of compensatory vasoconstriction through activation of sympathetic efferent pathways. Without such quick compensation, the simple act of standing would cause a fall in arterial pressure responsible for perfusing the brain, resulting potentially in loss of consciousness. Therefore, the characterization of dynamic, as well as static, properties of baroreflex function is vital for an understanding of its function.

A useful animal model for a variety of clinical diseases ranging from hypertension to heart failure, the rat is very important to cardiovascular research (4, 8, 24, 25, 28). Its usefulness in molecular-based investigations is also an important advantage (28). For these reasons, the physiology and pathophysiology of arterial baroreflex function have been frequently examined in rats under diseased as well as normal conditions. These studies, however, have been performed under closed-loop conditions due to inherent difficulties in the rat in isolating the baroreceptors and in opening the feedback loop. In such investigations, the pressure changes imposed on the baroreceptors were produced by the injections of vasoactive agents (4, 8, 12, 13, 16, 26) or blood (6). It is important to recognize that analyses of dynamic physiological systems under closed-loop conditions could lead to erroneous conclusions (14, 21). Specifically, the experimental preparations lacking strict controllability of the rate of pressure change could result in an erroneous estimation of baroreflex function. To overcome these limitations, we developed a new simple method for isolation of baroreceptor regions of the rat (20) and demonstrated the static characteristics of the baroreflex control of sympathetic efferent activity and arterial pressure (19). However, another important feature of baroreflex function of the rat, i.e., baroreflex dynamics, was not yet clarified. In rabbits, our previous study suggested a significance of derivative responses of sympathetic nerve activity (SNA) to change in baroreceptor pressure (BRP) in stabilization of arterial pressure (9). Bertram et al. (2) studied the frequency response of arterial pressure to electrical stimulation of the aortic depressor nerve of the rat, suggesting the significance of dynamic properties of the arterial baroreflex control of arterial pressure.

The purpose of this investigation was to characterize the dynamics of the baroreflex control of SNA and arterial pressure by a system identification method based on a white noise approach. The results provided the first and quantitative data on the dynamic charac-

Address for reprint requests and other correspondence: T. Sato, Dept. of Cardiovascular Control, Kochi Medical School, Nankoku, Kochi 783-8505, Japan (E-mail:tacsato-kochimed@umin.ac.jp).

The costs of publication of this article were defrayed in part by the payment of page charges. The article must therefore be hereby marked "*advertisement*" in accordance with 18 U.S.C. Section 1734 solely to indicate this fact.

teristics of the arterial baroreflex in rats and also suggested some limitations of the routine methods in estimation of so-called baroreflex sensitivity, i.e., the maximum gain of the baroreflex control of sympathetic nerve activity.

METHODS

Theoretical Consideration

We opened the feedback loop of the arterial baroreflex system and divided the system into its controlling element, mechanoneural arc, and its controlled element, neuromechanical arc. In the mechanoneural arc, the input is arterial BRP and the output is SNA. In the neuromechanical arc, the input is SNA, and the output is systemic arterial pressure (SAP). Inasmuch as the variables characterizing the functions of the two arcs are common, the operating point of the feedback system should be given as an intersection between them on an equilibrium diagram. Our previous study (19) showed that the two functional curves of the two arcs intersected each other at the point where the steady-state gain of each arc attained its maximum. Because each arc curve is significantly sigmoid shaped and the steady-state gain depends on the operating point, much attention should be paid to the design of the mean and range of BRP perturbation for estimation of baroreflex dynamics. Therefore, in the present study, to estimate the dynamics of each arc around the operating point, we first measured the operating point of the system and then designated the perturbation pressure imposed on the baroreceptors.

Animals and Surgical Procedures

The care of animals was in strict accordance with the "Guiding Principles for Research Involving Animals and Human Beings" of American Physiological Society (1). A total of 11 male Sprague-Dawley rats weighing 280–350 g were used. The rat was first placed in a glass jar where it inspired a mixture of 2% halothane (Fluothane; Takeda Pharmaceuticals, Tokyo, Japan) in oxygen-enriched air for 5–10 min. After the induction of anesthesia, an endotracheal tube was introduced orally, and the rat was ventilated artificially via a volume-controlled rodent respirator (model 683; Harvard Apparatus, South Natick, MA). The respiratory rate was controlled at 1.5 Hz. In accordance with Ono et al. (16), anesthesia was maintained through the use of 1.2% halothane during surgical procedures and 0.6% halothane during data recording. Polyethylene tubings (PE-10; Becton Dickinson, Parsippany, NJ) were inserted into the right femoral vein and the left common carotid artery. Pancuronium bromide (0.8 $mg \cdot kg^{-1} \cdot h^{-1}$ iv) was administered to eliminate spontaneous muscle activity. Arterial blood gases were monitored with a blood gas analyzer (IL-13064; Instrumentation Laboratory, Lexington, MA). For the prevention of dehydration during experiments, physiological saline was continuously infused at a rate of 5 $ml \cdot kg^{-1} \cdot h^{-1}$ with a syringe pump (CFV-3200; Nihon Kohden, Tokyo, Japan). For measurement of SAP, a 2-Fr catheter-tip micromanometer (SPC-320; Millar Instruments, Houston, TX) was placed in the aortic arch through the right femoral artery.

To open the feedback loop of the arterial baroreflex system, we cut the vagi and the aortic depressor nerves and isolated the carotid sinus baroreceptor regions by the embolization method (15, 20). In our previous study (20), we extensively described the surgical procedures for isolation of carotid sinus baroreceptors with ball bearings. Briefly, the external carotid artery was ligated at its root of the bifurcation of the common carotid artery, and then the internal carotid and pterygopalatine arteries were embolized with two ball bearings of 0.8 mm diameter. Two short polyethylene tubings (PE-50) were placed into both carotid sinuses and connected to a fluid-filled transducer (DX-200; Viggo-Spectramed, Singapore) and to a custom-made servo-controlled pump system (22, 23) based on an electromagnetic shaker and power amplifier (ARB-126; AR Brown, Osaka, Japan). We used the servo-controlled pump to impose various pressures on carotid sinus baroreceptor regions.

To record SNA, we identified the left renal nerve branch from the aorticorenal ganglion via a retroperitoneal approach through a left flank incision. The nerve branch was isolated, carefully dissected free, and cut. The central end of the nerve branch was placed on a pair of Teflon-coated platinum wires (7720; A-M Systems, Everette, WA). The implantation site of the wires was embedded in silicone rubber (Sil-Gel 604; Wacker, Munich, Germany). Finally, the flank incision was closed in layers. The nerve activity was amplified and bandpass filtered in the frequency range between 150 and 3,000 Hz (JB-610J and AB-610J; Nihon Kohden). The enveloped waveform of SNA was generated through a custom-made circuit with a cut-off frequency of 100 Hz (−3 dB).

Data Recording

Protocol 1: measurement of operating points under closed-loop conditions. To measure the operating points under the closed-loop conditions of the arterial baroreflex system, we closed the feedback loop of the system with our servo-controlled pump system. A dedicated laboratory computer (PC-9801RA21; NEC, Tokyo, Japan) in real time commanded the power amplifier to make carotid sinus BRP identical with SAP by means of a digital-to-analog converter (DA12-4-98; Contec, Osaka, Japan), while digitizing SAP at a rate of 2 kHz through a 12-bit analog-to-digital converter (AD12-16D-98H; Contec). Using this technique, we were able to impose the same pressure waveform as SAP on the carotid sinus baroreceptors in the frequency range up to 10 Hz. BRP, SNA, and SAP were recorded for 3 min under the closed-loop conditions.

Protocol 2: white noise system identification of mechanoneural and neuromechanical arcs. To estimate the transfer functions characterizing dynamic characteristics of the mechanoneural and neuromechanical arcs and the total arc, we used a white noise system identification method. We randomly altered BRP between the measured operating pressure of ±10 mmHg every 0.4 s. The electrical signals of BRP, SNA, and SAP were low-pass filtered with antialiasing filters having a cutoff frequency of 100 Hz (−3 dB) and an attenuation slope of −80 dB/decade (ASIP-0260L; Canopus, Kobe, Japan) and were then digitized at 200 Hz by means of the analog-to-digital converter for 1 h. To calibrate the level of SNA for each rat, we measured SNA at 80 and 160 mmHg of BRP and then recorded the background noise after the renal nerve was crushed between the aorticorenal ganglion and the recording site.

Data Analysis

Because the absolute voltage value of SNA depends on various physical recording conditions such as the size and positioning of the electrodes, we expressed the level of SNA in an arbitrary unit (au). For each rat, SNA was normalized by the values at 80 and 160 mmHg of BRP after the average background noise level was subtracted.

To characterize the dynamic properties of the mechanoneural, neuromechanical, and total arcs, we estimated the transfer functions from BRP to SNA, from SNA to SAP, and from BRP to SAP. The transfer function $H_{x\rightarrow y}$ from input x to output y was computed with a fast Fourier transform algorithm (14, 21–23). The digitized data of x and y were resampled at 20 Hz after a moving average. The time series of each data point was divided into 50 segments of 2,048 points each, with 1,024 points of overlap between segments. The length of each segment was 102.4 s in duration. To suppress spectral leakage, we applied a Hann window to each segment and then computed the raw autospectra of x and y and the raw cross-spectrum between the two. To reduce an error in estimating the spectrum, we calculated the ensemble average of 50 raw spectra. Finally, we computed the transfer function over the frequency range of 0.0098–1.25 Hz with a resolution band width of 0.0098 Hz as follows

$$H_{x\rightarrow y} = \frac{S_{xy}}{S_{xx}}$$

where S_{xx} is the ensembled autospectrum of x, and S_{xy} is the ensembled cross-spectrum of x and y. $H_{x\rightarrow y}$ is, in general, a complex quantity and is therefore expressible in polar form as

$$H_{x\rightarrow y} = |H_{x\rightarrow y}| \exp(j\phi_{x\rightarrow y})$$

where $j^2=-1$ and $|H_{x\rightarrow y}|$ and $\phi_{x\rightarrow y}$ are the gain and phase of the transfer function, respectively. The gain spectrum was normalized by its value at the lowest frequency. The squared coherence function, a measure of linear dependence between x and y, was estimated with the following equation

$$\text{coh} = \frac{|S_{xy}|^2}{S_{xx} \times S_{yy}}$$

where S_{yy} is the ensembled autospectrum of y.

The step response that represents a transient change in y in response to a sudden step increase in x was estimated by integration of the impulse response function computed from an inverse Fourier transform of the transfer function (14). The estimated step response had a resolution time interval of 0.4 s.

Values were expressed as means ± SD.

RESULTS

The arterial pressure at the operating point of the closed-loop system was 118 ± 5 mmHg for 11 rats. Shown in Fig. 1*A* is a representative example of original tracings of BRP, SNA, and SAP during random pressure perturbation to carotid sinus baroreceptors. An increase in BRP seems to rapidly suppress SNA and gradually lower SAP and vice versa. The power of change in BRP was fairly constant up to 1.25 Hz (Fig. 1*B*). Considering that the pressure perturbation with a bandwidth of interest (≤1.25 Hz) was prerequisite for the accurate and reliable estimation of the transfer functions from BRP to SNA and BRP to SAP, our perturbation seems to be sufficient and valid for estimation.

Shown in Fig. 2 are the averaged transfer functions and step responses from BRP to SNA, from SNA to SAP, and from BRP to SAP for 11 rats. The gain from input to output is normalized by the value at the lowest frequency, i.e., steady-state gain, showing the relative change in the gain in response to the change in the input frequency. The steady-state gain from BRP to SNA was 0.021 ± 0.003 au/mmHg, that from SNA to SAP was 98 ± 13 mmHg/au, and that from BRP to SAP was 2.5 ± 0.3. The gain of the mechanoneural arc gradually increased about threefold up to 0.8 Hz and then decreased with input frequencies (Fig. 2*A*). Whereas the phase spectrum shows that the input-output relationship was out of phase at steady state, a small but significant phase lead was found below 0.5 Hz. On the basis of these characteristics, the mechanoneural arc is considered as a filter with both derivative and high-cut characteristics. The normalized gain had a peak at 0.8 Hz and a phase change of π/2 over the frequency range. These properties of the mechanoneural arc are clearly indicated by the step response estimated from the transfer function. The

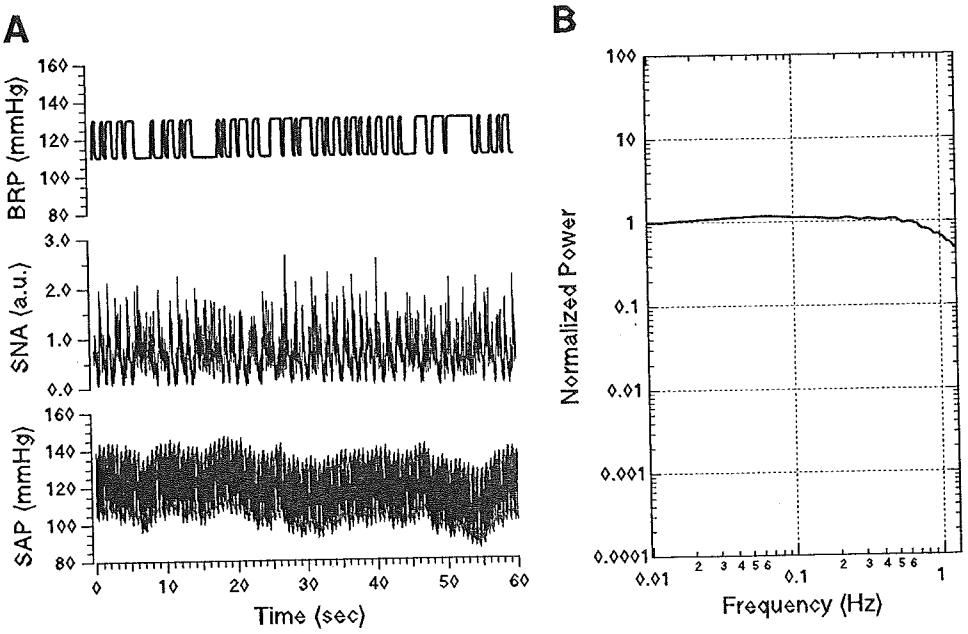

Fig. 1. Original tracings of carotid sinus baroreceptor pressure (BRP), sympathetic nerve activity (SNA), and systemic arterial pressure (SAP) during random BRP perturbation (*A*) and a power spectrum of change in BRP in the frequency range of 0.0098–1.25 Hz with a resolution bandwidth of 0.0098 Hz (*B*). Power was normalized by the value at the lowest frequency.

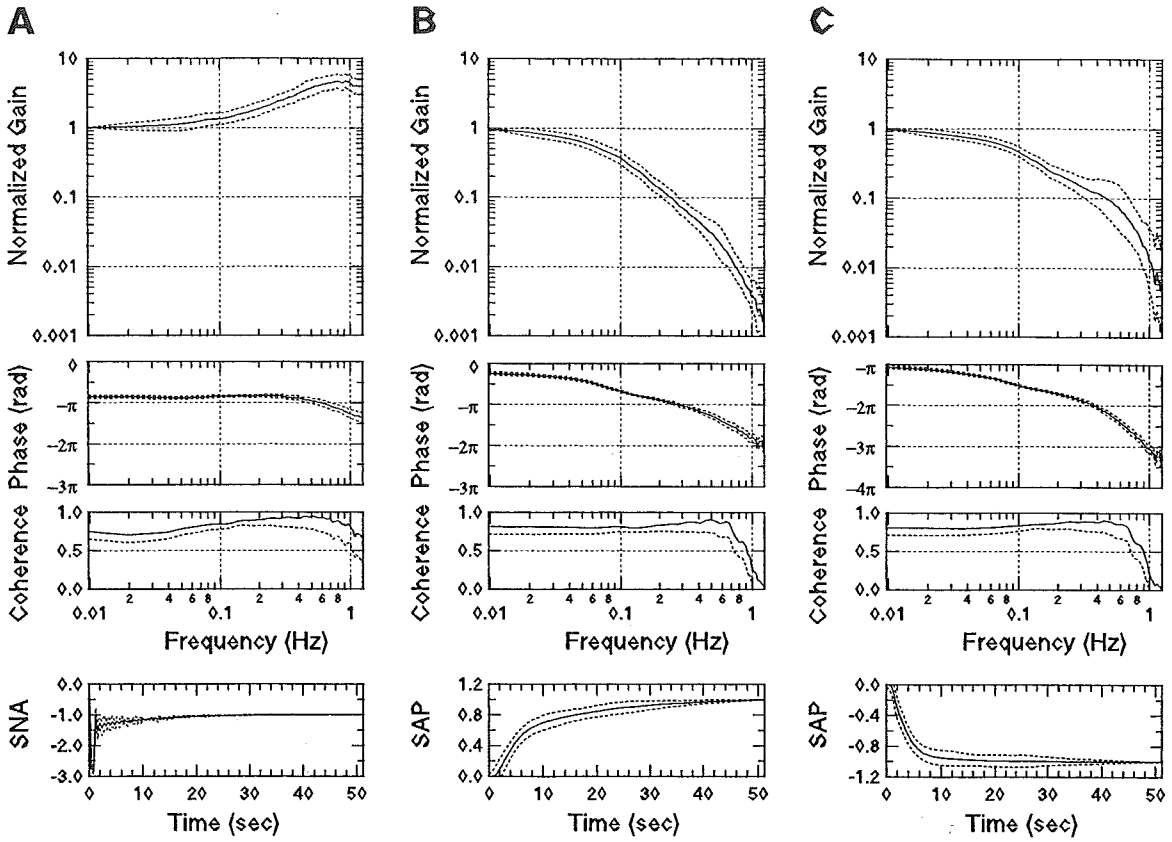

Fig. 2. Graphs showing averaged transfer functions and step responses from carotid sinus BRP to SNA (*A*), from SNA to SAP (*B*), and from BRP to SAP (*C*) in the frequency range of 0.0098–1.25 Hz with a resolution bandwidth of 0.0098 Hz for 11 rats. Dotted lines are means ± SD; in the coherence spectrum, data are expressed as means − SD. The gain was normalized by the value at the lowest frequency; the step response was normalized by its steady-state value. rad, Radians. See text for explanation.

SNA response to a step-wise increment in BRP exhibits an initial overshoot inhibition with the dead time of 0.12 ± 0.01 s (see APPENDIX for calculation of dead time). The response peaked at 0.4 s to −281 ± 13% of the steady-state value and then rapidly reached the steady-state value within 10 s. The gain of the neuromechanical arc rapidly decreased to 0.4% of the steady-state value as the frequency increased from 0.01 to 1 Hz (Fig. 2*B*). The phase shift increased with frequencies. These low-pass characteristics are clearly indicated by the step response estimated from the transfer function. The SAP exhibits a sluggish pressor response to a step-wise increment in SNA. The dead time was 0.68 ± 0.19 s, and the response reached 90% of the steady-state value at 25 ± 3 s. Similar to the neuromechanical arc, the total arc had low-pass characteristics (Fig. 2*C*). However, the rate of the gain attenuation of the total arc was significantly slower than that of the neuromechanical arc, reflecting the compensatory effect of the mechanoneural arc for the sluggish response of the neuromechanical arc. Such a difference was also clearly found in the step responses. Compared with the step response of the neuromechanical arc, that of the total arc was quick to attain the steady-state value; the elapsed time to reach 90% of the steady-state response was 7.2 ± 2 s (Fig. 2*C*, *bottom*). The dead time was 0.79 ± 0.21 s. It should be noted that the squared coherence value was close to unity up to 0.7 Hz. High coherence values suggested that the input-output relationships of the mechanoneural, neuromechanical, and total arcs were predominantly governed by linear dynamics and that the transfer functions and step responses well described the dynamic properties of the respective arcs of arterial baroreflex.

DISCUSSION

Using the previously developed methods for isolation of the baroreceptor region (20) and a white noise technique (14, 21), we systematically identified the dynamic properties of the baroreflex control of SNA and SAP in rats. To our knowledge, this is the first study showing the quantitative results of baroreflex dynamics in rats, which provide many important animal models for cardiovascular pathophysiology.

Open-Loop Approach

Bertram et al. (2) studied the frequency response of arterial pressure to electrical stimulation of the aortic depressor nerve of the rat, suggesting the significance of dynamic properties of the arterial baroreflex control of arterial pressure. They showed the transfer function

from the electrical stimulation of the left aortic depressor nerve to SAP under the intact conditions of both carotid sinus nerves and the right aortic depressor nerve. They also reported that denervation of both carotid sinus nerves and the right aortic depressor nerve had no significant effect on the characteristics of the transfer function. However, our previous work (10) tested the validity of the estimation of the transfer function using the random electrical stimulation of the aortic depressor nerve in rabbits, concluding that the unbiased or accurate transfer function could not be estimated if carotid sinus and/or aortic baroreceptor reflexes were functioning.

As shown in our previous study (19), baroreceptor transduction properties in rats exhibit a significant transient response. Therefore, our pressure loading method is more suitable for characterization of the arterial baroreflex control of SAP than the nerve stimulation method. In terms of systems physiology, for characterization of the feedback system, the input should be a feedback variable, i.e., BRP, and the output should be a controlled variable, i.e., SAP. According to the open-loop approach, we can characterize the most important function of the arterial baroreflex, i.e., total-loop dynamics.

Our experimental preparations for alternating between open- and closed-loop conditions of the baroreflex system even after isolation of baroreceptor regions and for servocontrolling BRP at any level allowed us to quantitatively evaluate the baroreflex dynamics in each animal. Our previous study (19) revealed that the effectiveness of baroreflex in attenuation of the effect of external disturbance depended on the operating point of the baroreflex system before the disturbance. Interestingly, the static open-loop gain from BRP to SAP was well optimized to be 2–3 at the operating point of the closed-loop system before the external perturbation, i.e., 110–130 mmHg. Such a relationship was also observed in the mechanoelectrical transduction properties of rat baroreceptors (20). Thus to clarify the physiological baroreflex dynamics, we should pay much attention to the design of BRP. In the present study, we carefully selected the level of BRP for each rat, so that the level was matched to the operating point of the closed-loop system at the baseline conditions.

System Identification by White Noise Approach

For characterization of the dynamic properties of the baroreflex control of SNA and SAP accurately and quantitatively, a white noise approach for system identification (14, 21) is more suitable than traditional methods with step and sine-wave stimuli. Because imposition of truly step-wise, i.e., with an infinitesimal rise and/or fall time, waveforms of pressure on baroreceptors is impossible (3), the accurate step response cannot be measured. Because of the limited input frequencies of sinusoidal waveforms of pressure, it would be difficult to accurately estimate the gain and phase characterizing the input-output relationship in the frequency domain (14, 21). In the white noise approach, the system is, on the other hand, tested with every possible stimulus and thus would be well characterized in the frequency domain. Moreover, the identification of the physiological system through the white noise technique is largely unaffected by the types of contaminating noise usually present in such a system (14).

The white noise method has another important advantage (14). If the transfer function of a system is accurately identified, we can estimate the impulse- and step-response functions. Thus we can quantitatively, in the time domain, visualize a transient response of the system and simulate the response to any waveform input in the frequency range of interest (21). These data help us understand the dynamics of the system.

Interestingly, arterial pressure of conscious rats (13, 15) changes within the BRP range used in the present study and the high coherence values are found in the input-output relationships of the mechanoneural and neuromechanical arcs and the total arc in this pressure range. Therefore, the arterial baroreflex system would be considered to be governed by linear dynamics under the physiological conditions.

Baroreflex Dynamics in Rat

Persson et al. (17) and Di Rienzo et al. (5) examined the influence of the baroreflex on the different spectral components of SAP variability through the broad-band spectral analysis of SAP fluctuations in dogs and cats before and after sinoaortic denervation, suggesting that the arterial baroreflex system has a limited control on SAP at higher frequencies. This suggestion was consistent with the present result that the gain of the total arc shown in Fig. 2*C* decreased progressively at higher frequencies. Petiot et al. (18) showed the transfer function from the electrical stimulation of the aortic depressor nerve to SNA in rats, indicating that the gain increases threefold at 0.8–1 Hz and the phase leads up to 0.5–0.6 Hz. Such characteristics seem to be similar to the transfer function from BRP to SNA shown in the present study. Therefore, the dynamic properties of the rat arterial baroreceptors are not apparent in this frequency range, which would accord with the findings by Brown et al. (3).

In our previous study (9), we examined the dynamic properties of the baroreflex control of SNA and SAP in rabbits. The derivative characteristics of the mechanoneural arc compensated the low-pass characteristics of the neuromechanical arc, and thus the closed-loop baroreflex control of SAP was optimally accelerated. The derivative characteristics of the mechanoneural arc shown in Fig. 2 would be important in optimization of the baroreflex control of SAP in rats as well as in rabbits.

To clarify the effect of the high-pass characteristics of the mechanoneural arc, we evaluated the difference in the transient responses of SAP to an external disturbance in pressure between the closed-loop systems with and without the derivative characteristics. Shown in Fig. 3*A* is a block diagram of the baroreflex feedback system. Under the closed-loop conditions, the effect of the external disturbance in pressure, ΔP_d, is attenu-

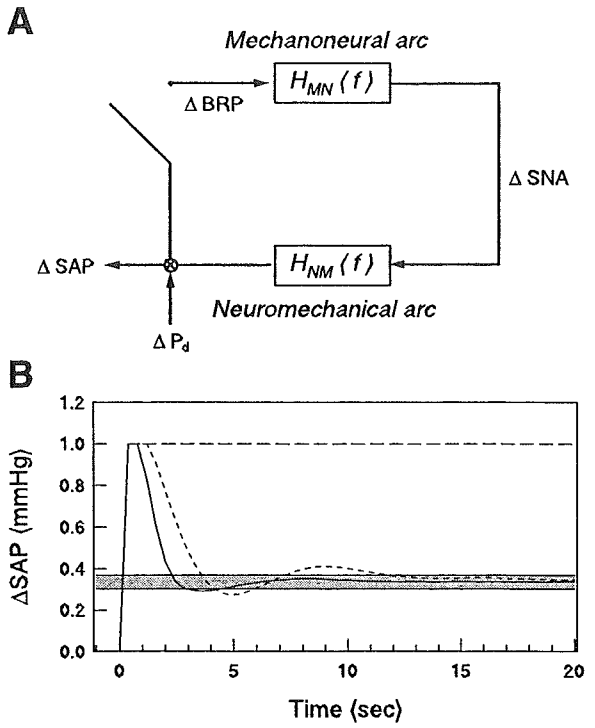

Fig. 3. *A*: block diagram of the sympathetic baroreflex feedback system. Under the closed-loop conditions, a change in BRP, ΔBRP, is the same as a change in SAP, ΔSAP, and thus the effect of an external disturbance in pressure, ΔP_d, is attenuated. $H_{MN}(f)$ and $H_{NM}(f)$ represent transfer functions of the mechanoneural and neuromechanical arcs. ΔSNA, change in SNA. *B*: graph showing the simulated results of ΔSAP in response to a step-wise ΔP_d. ΔP_d with a magnitude of 1 mmHg is imposed at 0 s. Under the open-loop conditions (dashed line), the effect of ΔP_d is not attenuated at all. Assuming that $H_{MN}(f)$ and $H_{NM}(f)$ are the averaged transfer functions of the respective arcs shown in Fig. 2, *B* and *C*, and that the steady-state gain of the total arc is 2, the effect of ΔP_d is attenuated to one-third at the steady state. The time for the peak attenuation is 3.6 s (solid line); the transient response converges within the range of ±10% of the steady-state response (shadow zone) in 4.4 s. However, if only $H_{MN}(f)$ is replaced by an all-pass filter with flat gain and phase characteristics, the underdamped oscillatory response becomes clear (dotted line). The time for the peak attenuation increases to 4.8 s; the time for the convergence within the range of ±10% of the steady-state response is prolonged to 11.6 s. See text for details.

ated, and thus the resultant change in SAP, ΔSAP, is represented in the frequency domain as follows

$$\Delta SAP(f) = \frac{\Delta P_d(f)}{1 - H_{MN}(f) \cdot H_{NM}(f)}$$

where $H_{MN}(f)$ and $H_{NM}(f)$ are the transfer functions of the mechanoneural and neuromechanical arcs, respectively. The time integral of the inverse Fourier transform of ΔSAP(f) reveals the time series of ΔSAP in response to a step-wise ΔP_d. If the feedback loop was opened, the effect of ΔP_d was not attenuated at all, and thus ΔSAP equaled ΔP_d (Fig. 3*B*, *dashed line*). Assuming that $H_{MN}(f)$ and $H_{NM}(f)$ were the averaged transfer functions of the respective arcs shown in Fig. 2, *B* and *C*, and that the steady-state gain of the total arc was 2, the effect of ΔP_d was attenuated to one-third at the steady state after damped oscillation. The time for the peak attenuation was 3.6 s; the transient response converged within the range of ±10% of the steady-state response in 4.4 s (Fig. 3*B*, *solid line*). However, if only $H_{MN}(f)$ was replaced by an all-pass filter with flat gain and phase characteristics, the underdamped oscillatory response became clearer (Fig. 3*B*, *dotted line*). The time for the peak attenuation increased to 4.8 s; the time for the convergence within the range of ±10% of the steady-state response was prolonged to 11.6 s. These results, therefore, suggest that the derivative characteristics of the mechanoneural arc significantly contribute to the quick and stable attenuation of the effect of the external disturbance on SAP.

In our previous study on the rabbit baroreflex system (9), the simulated response of the closed loop to step-wise pressure perturbation showed no oscillation of SAP, which is different from the present result. This inconsistency would result from the difference in animal species between these two studies. Another possibility is the difference in the value of the total arc gain (19). The gain estimated in the previous study was less than one-half of the value obtained in the present study. The difference in the estimated value for the baroreflex gain could be ascribed to the difference in the level of BRP used for transfer function analysis. In the previous study (9), the mean level of BRP was quite different from that of SAP (75 vs. 128 mmHg). Thus the level of BRP was not matched to the operating point of the closed-loop system. As discussed in *Open-Loop Approach*, this mismatching could produce the underestimation of the total arc gain. Therefore, to clarify how dynamically the baroreflex system attenuates the effect of an external disturbance under the closed-loop conditions, we should carefully design BRP.

Implications for Baroreflex Studies in Nonisolated Preparations

Many studies concerning baroreflex function mediated by the arterial baroreceptors have been conducted under closed-loop conditions in rats. Ramp changes in arterial pressure were routinely produced by the injections of vasoactive agents (4, 8, 12, 13, 16, 26) and blood (6). The rate of BRP change could not be strictly controlled under such conditions, and thus the results would be inconsistent and imprecise. The rates of BRP change induced by the conventional methods were considerably different (0.28–10 mmHg/s) among these studies; a large difference in the rate was found even within individual studies. The effect of the rate of BRP change, however, has never been evaluated quantitatively.

To clarify the effect of the rate of a ramp BRP change on a widespread index for baroreflex function, baroreflex sensitivity (BRS), we performed a simulation study. Using a convolution algorithm (14, 21) and the representative impulse-response function h(t) computed by an inverse Fourier transform of the transfer function estimated in the present study, we simulated the responses of SNA $y(t)$ to ramp BRP changes $x(t)$ with different rates (0.5–10 mmHg/s, every 0.5 mmHg/s)

$$y(t) = \int_0^\infty h(\tau) \cdot x(t - \tau) d\tau$$

The examples of simulated results of time-series data of SNA responses to ramp BRP rises and falls at the rates of 0.5 and 10 mmHg/s are presented in Fig. 4, *A* and *B*. For these cases, we plotted the instantaneous responses of SNA to changes in BRP (Fig. 4*C*). The BRS value, i.e., the maximum slope estimated from the instantaneous SNA response curve, obviously depends on the rate of BRP change. Figure 4*D* indicates the relationship between the estimates for the BRS and the rates of BRP change, suggesting that the BRS value is inevitably overstimulated during the faster ramp change in BRP. Therefore, the BRS should be recognized as a function of the rate of BRP change and should be redefined as the maximum gain at a specific rate of BRP change. From these results, we conclude that the strict control of the rate of BRP change is vital for the accurate and reliable evaluation of baroreflex function, because of baroreflex dynamics.

Limitations

As shown in Fig. 2, the gain values from SNA to SAP and from BRP to SAP were pretty small at the higher frequencies over 0.7 Hz. We used a 12-bit analog-to-digital converter for data acquisition of electrical signals of ±5 V. The signal of arterial pressure was amplified to be 0 V for 0 mmHg and 5 V for 250 mmHg. Therefore, an error in quantization, i.e., a signal resolution, was 0.12 mmHg. These limitations affected coherence values. For example, if we imposed changes in BRP with an amplitude of 20 mmHg, and if the absolute gain values of the total arc at 0.01 and 1 Hz were 2 and 0.01, respectively, the measured changes in SAP at 0.01 and 1 Hz should be 40 and 0.2 mmHg, respectively. It is difficult to accurately measure a change of 0.2 mmHg using our system. Therefore, lower coherence values at the higher frequencies in the transfer functions of the neuromechanical and total arcs would result from the lower signal-to-noise ratio.

The purpose of this study was to characterize the arterial baroreceptor reflex with carotid sinus baroreceptor afferent and the sympathetic efferent limbs. Therefore, for the sake of simplicity, we bilaterally cut the vagal nerves to exclude the effect of cardiopulmonary receptors (7, 17) and the vagal control of heart rate. Because of difficulty in the control of aortic baroreceptor pressure, we also cut the aortic depressor nerves to open the arterial baroreflex loop. Therefore, in the present study, we could characterize the dynamic properties of the arterial baroreceptor reflex with carotid sinus baroreceptor afferent and the sympathetic efferent limbs. Thus the transfer function of the mechanoneural arc did not include the effect of the baroreceptors of the aortic depressor nerve. It is noted that the transfer function of the neuromechanical arc reflected the dynamic properties of the sympathetic

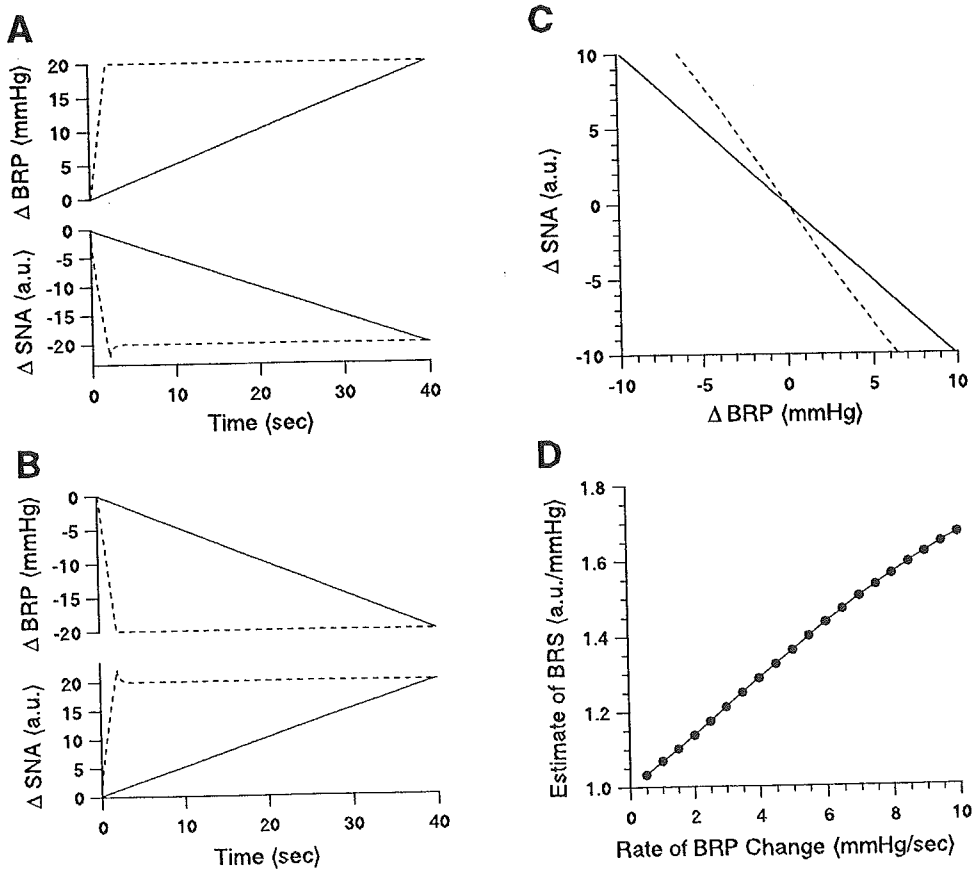

Fig. 4. Graphs showing the simulated responses of SNA to ramp rises (*A*) and falls (*B*) in BRP at the rates of 0.5 (*solid line*) and 10 (*dotted line*) mmHg/s, and the instantaneous relationship between changes in BRP and SNA (*C*). *D*: graph showing the relationship between the baroreflex sensitivity (BRS) estimated from the instantaneous response curve and the rate of BRP change. au, Arbitrary units. See text for details.

modulation of not only vascular but also cardiac characteristics such as heart rate and cardiac contractility.

Anesthetic agents used in the present study could also affect the dynamic properties of arterial baroreflex. The vasomotor center of the arterial baroreflex is affected by higher-order centers such as the limbic-hypothalamic systems and also receives various afferents from the periphery such as sympathetic afferent cardiac and splanchnic fibers. In the present study, we ignored these components. Thus further investigation concerning the effects of these components is needed for clarifying the dynamics of arterial baroreflex.

In conclusion, we characterized the dynamic properties of the mechanoneural, neuromechanical, and total arcs of the arterial baroreflex of the rat by the white noise system identification method. The derivative nature of the mechanoneural arc compensated for the sluggish response of the neuromechanical arc, and thus the total arc response was significantly accelerated. The simulated result with the transfer function of the mechanoneural arc suggested that the apparent maximum gain estimated from the instantaneous relationship between BRP and SNA, i.e., baroreflex sensitivity, depended on the rate of change in BRP because of the dynamic nature of the mechanoneural arc. We conclude that the quantitative estimation of the dynamic characteristics of arterial baroreflex is vital for an understanding of baroreflex function and that the routine methods lacking strict controllability of the rate of BRP change could result in erroneous conclusions.

APPENDIX

As described previously (11), we could model the transfer function of the mechanoneural arc as follows

$$H_{MN}(f) = -\frac{1 + \left(\frac{f}{f_{MN1}}\right)j}{\left(1 + \frac{f}{f_{MN2}}j\right)^2} \exp(-2\pi f j L_{MN})$$

where f and j represent the frequency (in Hz) and imaginary units, respectively; f_{MN1} and f_{MN2} ($f_{MN1} < f_{MN2}$) are corner frequencies for derivative and high-cut characteristics, respectively; and L_{MN} is a pure delay or dead time (in s). When f_{MN2} is set greater than f_{MN1}, dynamic gain increases in the frequency range from f_{MN1} to f_{MN2} and decreases above f_{MN2}. When f_{MN2} is far greater than the frequency range of interest, $H_{MN}(f)$ approximates a derivative filter. The phase shift due to derivative and high-cut filters and the pure delay yield the overall phase characteristics. Introduction of the pure dead time L_{MN} would be reasonable because the baroreceptor transduction, nerve conduction, and synaptic transmission should be assumed in the transfer function from BRP and SNA.

Similarly, we could model the transfer function of the neuromechanical arc with a second-order low-pass filter as follows

$$H_{NM}(f) = \frac{1}{1 + 2\zeta\left(\frac{f}{f_{NM}}\right)j + \left(\frac{f}{f_{NM}}j\right)^2} \exp(-2\pi f j L_{NM})$$

where f_{NM} and ζ indicate a natural frequency and a damping ratio, respectively. The pure delay L_{NM} would be due to the electromechanical transduction from SNA to SAP.

The transfer function of the total arc could be modeled as the product of $H_{MN}(f)$ and $H_{NM}(f)$. Finally, the dead time of the total arc was calculated from the sum of L_{MN} and L_{NM}.

This study was supported by the Grant-in-Aid for Scientific Research (11680862) from the Ministry of Education, Science, Sports, and Culture of Japan, by the Health Sciences Research Grant for Advanced Medical Technology (H10-003-FY1997) from the Ministry of Health and Welfare of Japan, by the Ground Research Grant for Space Utilization from the National Space Development Agency of Japan and Japan Space Forum, and by grants from Uehara Memorial Foundation, Suzuken Memorial Foundation, Tateisi Science and Technology Foundation, and Mochida Memorial Foundation.

REFERENCES

1. **American Physiological Society.** Guiding principles for research involving animals and human beings. *Am J Physiol Regul Integr Comp Physiol* 283: R281–R283, 2002.
2. **Bertram D, Barrès C, Cuisnaud G, and Julien C.** The arterial baroreceptor reflex of the rat exhibits positive feedback properties at the frequency of Mayer waves. *J Physiol* 513: 251–261, 1998.
3. **Brown AM, Saum WR, and Tuley FH.** A comparison of baroreceptor discharge in normotensive and spontaneously hypertensive rats. *Circ Res* 39: 488–496, 1976.
4. **DiBona GF and Sawin LL.** Reflex regulation of renal nerve activity in cardiac failure. *Am J Physiol Regul Integr Comp Physiol* 266: R27–R39, 1994.
5. **Di Rienzo M, Castiglioni P, Parati G, Mancia G, and Pedotti A.** Effects of sino-aortic denervation on spectral characteristics of blood pressure and pulse interval variability: a wide-band approach. *Med Biol Eng Comput* 34: 133–141, 1996.
6. **Dos Santos CM, Moreira ED, Krieger EM, and Michelini LC.** Chronic AT_1 receptor blockade alters aortic nerve activity in hypertension. *Hypertension* 31: 973–977, 1998.
7. **Floras JS, Butler GC, Ando S, Books SC, Pollard M, and Picton P.** Differential sympathetic nerve and heart rate spectral effects of nonhypotensive lower body negative pressure. *Am J Physiol Regul Integr Comp Physiol* 280: R468–R475, 2001.
8. **Huang BS, Yuan B, and Leenen FHH.** Blockade of brain "ouabain" prevents the impairment of baroreflexes in rats after myocardial infarction. *Circulation* 96: 1654–1659, 1997.
9. **Ikeda Y, Kawada T, Sugimachi M, Kawaguchi O, Shishido T, Sato T, Miyano H, Matsuura W, Alexander J Jr, and Sunagawa K.** Neural arc of baroreflex optimizes dynamic pressure regulation in achieving both stability and quickness. *Am J Physiol Heart Circ Physiol* 271: H882–H890, 1996.
10. **Kawada T, Sato T, Inagaki M, Shishido T, Tatewaki T, Yanagiya Y, Zheng C, Sugimachi M, and Sunagawa K.** Closed-loop identification of carotid sinus baroreflex transfer characteristics using electrical stimulation. *Jpn J Physiol* 50: 371–380, 2000.
11. **Kawada T, Zheng C, Yanagiya Y, Uemura K, Miyamoto T, Inagaki M, Shishido T, Sugimachi M, and Sunagawa K.** High-cut characteristics of the baroreflex neural arc preserve baroreflex gain against pulsatile pressure. *Am J Physiol Heart Circ Physiol* 282: H1149–H1156, 2002.
12. **Kumagai H, Averill DB, Khosla MC, and Ferrario CM.** Role of nitric oxide and angiotensin II in the regulation of sympathetic nerve activity in spontaneously hypertensive rats. *Hypertension* 21: 476–484, 1993.
13. **Kumagai K, Suzuki H, Ryuzaki M, Kumagai H, Ichikawa M, Jimbo M, Matsumura Y, and Saruta T.** Effects of antihypertensive agents on arterial baroreceptor reflexes in conscious rats. *Hypertension* 20: 701–709, 1992.
14. **Marmarelis PZ and Marmarelis VZ.** *Analysis of Physiological Systems: The White-Noise Approach.* New York: Plenum; 1978.
15. **McKeown KP and Shoukas AA.** Chronic isolation of carotid sinus baroreceptor region in conscious normotensive and hypertensive rats. *Am J Physiol Heart Circ Physiol* 275: H322–H329, 1998.
16. **Ono A, Kuwaki T, Kumada M, and Fujita T.** Differential central modulation of the baroreflex by salt loading in normo-

tensive and spontaneously hypertensive rats. *Hypertension* 29: 808–814, 1997.
17. **Persson PB, Ehmke H, Kohler WW, and Kirchheim HR.** Identification of major slow blood pressure oscillations in conscious dogs. *Am J Physiol Heart Circ Physiol* 259: H1050–H1055, 1990.
18. **Petiot E, Barrès C, Chapuis B, and Julien C.** Frequency response of renal sympathetic nervous activity to aortic depressor nerve stimulation in the anaesthetized rat. *J Physiol* 537: 949–959, 2001.
19. **Sato T, Kawada T, Inagaki M, Shishido T, Takaki H, Sugimachi M, and Sunagawa K.** New analytic framework for understanding sympathetic baroreflex control of arterial pressure. *Am J Physiol Heart Circ Physiol* 276: H2251–H2261, 1999.
20. **Sato T, Kawada T, Miyano H, Shishido T, Inagaki M, Yoshimura R, Tatewaki T, Sugimachi M, Alexander J Jr, and Sunagawa K.** New simple methods for isolating baroreceptor regions of carotid sinus and aortic depressor nerves in rats. *Am J Physiol Heart Circ Physiol* 276: H326–H332, 1999.
21. **Sato T, Kawada T, Shishido T, Miyano H, Inagaki M, Miyashita H, Sugimachi M, Knuepfer MM, and Sunagawa K.** Dynamic transduction properties of in situ baroreceptors of rabbit aortic depressor nerve. *Am J Physiol Heart Circ Physiol* 274: H358–H365, 1998.
22. **Sato T, Kawada T, Shishido T, Sugimachi M, Alexander J Jr, and Sunagawa K.** Novel therapeutic strategy against central baroreflex failure: a bionic baroreflex system. *Circulation* 100: 299–304, 1999.
23. **Sato T, Kawada T, Sugimachi M, and Sunagawa K.** Bionic technology revitalizes baroreflex function in rats with baroreflex failure. *Circulation* 106: 730–734, 2002.
24. **Sato T, Shishido T, Kawada T, Miyano H, Miyashita H, Inagaki M, Sugimachi M, and Sunagawa K.** ESPVR of in situ rat left ventricle shows contractility-dependent curvilinearity. *Am J Physiol Heart Circ Physiol* 274: H1429–H1434, 1998.
25. **Sato T, Yoshimura R, Kawada T, Shishido T, Miyano H, Sugimachi M, and Sunagawa K.** The brain is a possible target for an angiotensin-converting enzyme inhibitor in the treatment of chronic heart failure. *J Card Fail* 4: 139–144, 1998.
26. **Scheuer DA and Mifflin SW.** Glucocorticoids modulate baroreflex control of renal sympathetic nerve activity. *Am J Physiol Regul Integr Comp Physiol* 280: R1440–R1449, 2001.
27. **Thrasher TN and Shifflett C.** Effect of carotid or aortic baroreceptor denervation on arterial pressure during hemorrhage in conscious dogs. *Am J Physiol Regul Integr Comp Physiol* 280: R1642–R1649, 2001.
28. **Yoshimura R, Sato T, Kawada T, Shishido T, Inagaki M, Miyano H, Nakahara T, Miyashita H, Takaki H, Tatewaki T, Yanagiya Y, Sugimachi M, and Sunagawa K.** Increased brain angiotensin receptor in rats with chronic high-output heart failure. *J Card Fail* 6: 66–72, 2000.

Circ J 2003; **67:** 876–880

Biphasic Response of Action Potential Duration to Sudden Sympathetic Stimulation in Anesthetized Cats

Teiji Tatewaki, MD; Masashi Inagaki, MD; Toru Kawada, MD; Toshiaki Shishido, MD; Yusuke Yanagiya, PhD; Hiroshi Takaki, MD; Takayuki Sato, MD; Masaru Sugimachi, MD; Kenji Sunagawa, MD

Although certain roles of the sympathetic nervous system have been suggested as possible mechanisms of life-threatening arrhythmias and sudden cardiac death, the dynamic electrophysiological response to sympathetic activation remains unclear. The aim of this study was to investigate the dynamic response of action potential duration (APD) to sudden sympathetic stimulation (SYM) using monophasic action potential (MAP) recording. In 10 anesthetized cats, MAPs were continuously recorded from the right ventricular endocardium under constant pacing. The dynamic response of the APD to SYM (3 Hz) were examined before and after the administration of propranolol (0.5 mg/kg iv) (n=5) or phentolamine (1.0 mg/kg iv) (n=5). In response to SYM, the APD was transiently prolonged by 5.5±3.2 ms at 7.0±1.3 s, and monotonically shortened toward a steady-state level (−14.5± 6.9 ms). Propranolol almost abolished both the transient prolongation (6.6±4.5 to 0.2±0.4 ms, $p<0.05$) and the steady-state shortening (−13.7±3.6 to −1.1±2.4 ms, $p<0.005$), whereas phentolamine did not have a significant effect on the response of APD to SYM. These findings might partly account for the propensity of ventricular arrhythmias to occur immediately after sudden sympathetic activation. (*Circ J* 2003; **67:** 876–880)

Key Words: Action potential duration; Autonomic nervous system; Ventricular arrhythmias

Despite the tremendous progress in clinical cardiology, sudden cardiac death remains a major unsolved clinical issue[1,2] As possible mechanisms of sudden cardiac death, certain roles of the sympathetic nervous system have been suggested because there is ample experimental, clinical and therapeutic evidence to support the hypothesis that sympathetic hyperactivity favors the onset of life-threatening arrhythmias[3–6] A number of studies have examined how sympathetic nerve activation modulates the electrophysiological characteristics of the heart, especially ventricular repolarization. A shortening of the action potential duration (APD)[7] and refractory period[8,9] following sympathetic nerve stimulation have been reported.

Sudden stress is known to immediately evoke life-threatening arrhythmias in subjects who have certain predisposing conditions[3,10,11] suggesting that sudden sympathetic activation can abruptly render the heart vulnerable. Most previous studies, however, have focused on the steady-state electrophysiological response of the heart to sympathetic activation and the transient electrophysiological response to sympathetic activation remains unclear. In the present study, therefore, we investigated the dynamic response of APD to sudden sympathetic stimulation using monophasic action potential (MAP) recording.

Methods

Animal Preparation

Animal care was in accordance with the 'Guideline Principles for the Care and Use of Animals in the Field of Physiological Science' approved by Physiological Society of Japan. Experiments were performed on 10 cats of both sexes weighing 2.2–3.8 kg. The cats were anesthetized by intraperitoneal injection of pentobarbital sodium (30–35 mg/kg) and additional anesthetic (pentobarbital sodium 2.0 mg) was injected intravenously as needed to maintain the appropriate level of anesthesia. Cats were intubated using a cuffed endotracheal tube and mechanically ventilated with oxygenated air using a constant volume cycled respirator (Model SN-480-3, Shinano Inc, Tokyo, Japan). Polyethylene catheters were inserted into the femoral artery and vein for blood pressure (BP) recording and administration of fluids and drugs. Physiological saline was infused at a rate of 5 ml/h to replace spontaneous fluid loss. Each cat was placed on a heating pad. Throughout the experiment, body temperature, arterial blood gases and pH were maintained within their respective physiological ranges.

A midline cervical incision was made and the bilateral vagal nerves were identified and were severed to eliminate the vagal effects on the heart. Right and left stellate ganglia were exposed by removing part of the second rib on either side and were carefully isolated from the surrounding tissue. The proximal and distal connections were cut to decentralize each ganglion. A pair of platinum electrodes was attached to each of the cardiac sympathetic nerves to provide electrical stimulation. To prevent drying and to provide insulation, the stimulation electrodes and nerves were soaked in a mixture of white petrolatum (Vaseline) and liquid paraffin. The heart was exposed through a midsternotomy and was suspended in a pericardial cradle. A pair of bipolar electrodes was attached to the right ventricular apex for ventricular pacing. When atrioventricular dissociation was present during ventricular pacing, the right atrium was paced simultaneously to prevent competition for ventricular capture. The heart was paced at a constant rate

(Received March 10, 2003; revised manuscript received July 8, 2003; accepted July 24, 2003)

Department of Cardiovascular Dynamics, National Cardiovascular Center Research Institute, Suita, Japan
Mailing address: Teiji Tatewaki, MD, Department of Cardiovascular Dynamics, National Cardiovascular Center Research Institute, 5-7-1 Fujishirodai, Suita 565-8565, Japan